Fast Ewald summation for electrostatic systems with charges and dipoles for various types of periodic boundary conditions

Franziska Nestler
Chemnitz University of Technology
Faculty of Mathematics
09107 Chemnitz, Germany
Email: franziska.nestler@mathematik.tu-chemnitz.de

***Abstract*—The efficient computation of interactions in charged particle systems is possible based on the well known Ewald summation formulas and the fast Fourier transform for nonequispaced data (NFFT). The resulting method is known as the particle-particle NFFT (P^{2}NFFT) and has recently been generalized in order to consider electrostatic systems containing charges as well as dipole particles. The software is publicly available and supports various types of periodic as well as open boundary conditions. In this paper we give a short introduction to the method and present for the first time numerical results for mixed periodic and open boundary conditions.**

I. Introduction

We consider electrostatic systems with N_c point charges with charge values $q_j \in \mathbb{R}$, $j = 1,\dots,N_\mathrm{c}$, and N_d point dipoles with dipole moments $\boldsymbol{\mu}_j \in \mathbb{R}^3$, $j = N_\mathrm{c}+1,\dots,N_\mathrm{c}+N_\mathrm{d}$. The overall number of particles is denoted by $N := N_\mathrm{c}+N_\mathrm{d}$ and the positions of the particles are indicated by $\boldsymbol{x}_j \in [-L_1/2, L_1/2) \times [-L_2/2, L_2/2) \times [-L_3/2, L_3/2) \subset \mathbb{R}^3$, $j = 1,\dots,N$. In other words, we assume the particles to be distributed in a box with edge lengths $L_1, L_2, L_3 > 0$.

The total electrostatic energy U as well as the potentials $\phi(j)$ of the single particles subject to periodic boundary conditions are given, in Gaussian units, by

$$U := \frac{1}{2}\sum_{j=1}^{N} \xi_j \phi(j), \quad \phi(j) := \sum_{\boldsymbol{n}\in\mathcal{S}} {\sum_{i=1}^{N}}' \frac{\xi_i}{\|\boldsymbol{x}_{ij}+\boldsymbol{L}\boldsymbol{n}\|}. \quad (1)$$

The index set $\mathcal{S} \subset \mathbb{Z}^3$ is representing the applied periodic boundary conditions, the difference vectors $\boldsymbol{x}_{ij}$ are defined via $\boldsymbol{x}_{ij} := \boldsymbol{x}_i - \boldsymbol{x}_j$ and the prime on the double sum indicates that for $\boldsymbol{n} = \boldsymbol{0}$ all terms with $i = j$ are omitted, i.e., each particle is not allowed to interact with itself.

Furthermore, the term $\boldsymbol{L}\boldsymbol{n}$ denotes a matrix vector product, where the matrix $\boldsymbol{L} \in \mathbb{R}^{3\times 3}$ is a diagonal matrix with entries L_1, L_2, L_3, i.e., $\boldsymbol{L} = \mathrm{diag}(L_1, L_2, L_3)$, and the operators ξ_j are defined via $\xi_j := q_j$ for $j = 1,\dots,N_\mathrm{c}$ and $\xi_j := \boldsymbol{\mu}_j^\top \nabla_{\boldsymbol{x}_j}$ for all $j = N_\mathrm{c}+1,\dots,N$, cf. [1], where ∇ denotes the usual gradient operator.

If we assume periodic boundary conditions with respect to the first $p \in \{0,1,2,3\}$ dimensions and open boundary conditions regarding the last $3-p$ coordinates, we have to set $\mathcal{S} := \mathbb{Z}^p \times \{0\}^{3-p}$. The efficient computation of the introduced electrostatic quantities is required in the field of molecular dynamics simulations, for instance. In many applications periodic boundary conditions are assumed in order to avoid undesirable boundary effects, which would especially dominate in case of small systems sizes. On the other hand, in certain applications the focus is set on the investigation of such boundary effects. In order to simulate thin liquid films or nano channels, for instance, periodicity is only reasonable in two or one direction, respectively.

Note that the summands in (1) tend to zero like $\mathcal{O}(\|\boldsymbol{L}\boldsymbol{n}\|^{-1})$. Consequently, the series is only converging under certain conditions. One can show that if the system is charge neutral, i.e., we have $q_1 + \dots + q_{N_\mathrm{c}} = 0$, the series is conditionally convergent, i.e., the values of the different quantities strongly depend on the applied order of summation. Usually, a spherical summation order is applied, i.e., entire boxes are added by increasing norm of the corresponding lattice vectors $\|\boldsymbol{L}\boldsymbol{n}\|$, see [1] for instance.

In the field of molecular dynamics simulations one is also interested in the computation of the acting forces

$$\boldsymbol{F}(j) := \begin{cases} -q_j \nabla_{\boldsymbol{x}_j}\phi(j) & : j = 1,\dots,N_\mathrm{c}, \\ -\left[\nabla_{\boldsymbol{x}_j}\nabla_{\boldsymbol{x}_j}^\top \phi(j)\right]\boldsymbol{\mu}_j & : j = N_\mathrm{c}+1,\dots,N, \end{cases} \quad (2)$$

for which we need to calculate the partial derivatives of the potentials up to second order.

II. Ewald summation

The efficient computation of the electrostatic interactions is by no means straight forward, since the underlying sums are badly convergent. Note that in addition the interaction kernel $\|\boldsymbol{x}\|^{-1}$ and its derivatives have a singularity at $\boldsymbol{x} = \boldsymbol{0}$.

A large number of algorithms in the field of molecular dynamics simulations make therefore use of the so called Ewald summation technique [2]. Thereby, the Ewald splitting

$$\frac{1}{r} = \frac{\mathrm{erfc}(\alpha r)}{r} + \frac{\mathrm{erf}(\alpha r)}{r}, \quad (3)$$

is used, where α is called Ewald or splitting parameter, $\mathrm{erf}(x) := 2\pi^{-1/2}\int_0^x \mathrm{e}^{-t^2}\,\mathrm{d}t$ is the well known error function and $\mathrm{erfc}(x) := 1-\mathrm{erf}(x)$ is the complementary error function.

Note that the second term has a finite limit for $r \to 0$, which is given by

$$\lim_{r\to 0} \frac{\operatorname{erf}(\alpha r)}{r} = \frac{2\alpha}{\sqrt{\pi}}.$$

In other words, the second kernel function is continuous, but still converging to zero very slowly as $r \to \infty$. The complementary error function, in contrast, tends to zero exponentially fast with growing distance r, but still has a singularity in $r = 0$.

In summary, we end up with the following partition of the potentials $\phi(j)$ by applying the Ewald splitting (3).

$$\phi(j) = \phi^{\text{short}}(j) + \phi^{\text{long}}(j) + \phi^{\text{self}}(j),$$

where

$$\phi^{\text{short}}(j) := \sum_{\boldsymbol{n}\in\mathcal{S}} {\sum_{i=1}^{N}}' \xi_i \frac{\operatorname{erfc}(\alpha\|\boldsymbol{x}_{ij} + \boldsymbol{L}\boldsymbol{n}\|)}{\|\boldsymbol{x}_{ij} + \boldsymbol{L}\boldsymbol{n}\|}, \tag{4}$$

$$\phi^{\text{long}}(j) := \sum_{\boldsymbol{n}\in\mathcal{S}} \sum_{i=1}^{N} \xi_i \frac{\operatorname{erf}(\alpha\|\boldsymbol{x}_{ij} + \boldsymbol{L}\boldsymbol{n}\|)}{\|\boldsymbol{x}_{ij} + \boldsymbol{L}\boldsymbol{n}\|},$$

and

$$\phi^{\text{self}}(j) = \begin{cases} -\frac{2\alpha}{\sqrt{\pi}} q_j & : j = 1, \dots, N_{\text{c}}, \\ 0 & : j = N_{\text{c}} + 1, \dots, N. \end{cases} \tag{5}$$

The long range part is still badly converging, but the underlying kernel function is smooth and continuous, even at $\|\boldsymbol{x}_{ij} + \boldsymbol{L}\boldsymbol{n}\| = 0$. Thus, this part can be transformed into Fourier space with respect to all periodic dimensions. Of course, fundamentally different results are obtained for the different types of periodic boundary conditions.

A. 3d-periodic boundary conditions

If periodic boundary conditions are applied in all three dimensions, we set $\mathcal{S} := \mathbb{Z}^3 \iff p = 3$. In the following we denote by $V := L_1 L_2 L_3$ the volume of the primary box. Transforming the long range part into Fourier space based on the spherical summation order gives

$$\phi^{\text{long}}(j) = \sum_{\boldsymbol{k}\in\mathbb{Z}^3} \hat{\psi}(\boldsymbol{k}) S(\boldsymbol{k}) \, \mathrm{e}^{-2\pi \mathrm{i} \boldsymbol{k}^\top \boldsymbol{L}^{-1} \boldsymbol{x}_j} - \frac{2\pi}{3V} \sum_{i=1}^{N} \xi_i \|\boldsymbol{x}_{ij}\|^2 \tag{6}$$

with the Fourier coefficients

$$\hat{\psi}(\boldsymbol{k}) := \begin{cases} \dfrac{\mathrm{e}^{-\pi^2 \|\boldsymbol{L}^{-1}\boldsymbol{k}\|^2/\alpha^2}}{\pi V \|\boldsymbol{L}^{-1}\boldsymbol{k}\|^2} & : \boldsymbol{k} \neq \boldsymbol{0}, \\ 0 & : \boldsymbol{k} = \boldsymbol{0}, \end{cases}$$

and the structure factors

$$S(\boldsymbol{k}) := \sum_{i=1}^{N_{\text{c}}} q_i \, \mathrm{e}^{2\pi \mathrm{i} \boldsymbol{k}^\top \boldsymbol{L}^{-1} \boldsymbol{x}_i} + \sum_{i=N_{\text{c}}+1}^{N} \boldsymbol{\mu}_i^\top \nabla_{\boldsymbol{x}_i} \, \mathrm{e}^{2\pi \mathrm{i} \boldsymbol{k}^\top \boldsymbol{L}^{-1} \boldsymbol{x}_i}. \tag{7}$$

The result is obtained by applying the Poisson summation formula, cf. [2] and [1].

The Fourier coefficients $\hat{\psi}(\boldsymbol{k})$ tend to zero exponentially fast for growing $\boldsymbol{k}$, i.e., the obtained Fourier series in (6) can be approximated efficiently via truncation. The computation of the second term in (6) is straight forward due to charge neutrality, see [1], [3].

B. 2d-periodic boundary conditions

For 2d-periodic boundary conditions in the first two dimensions we have $\mathcal{S} := \mathbb{Z}^2 \times \{0\} \iff p = 2$. Within this section we denote by $\tilde{\boldsymbol{x}}_j := (x_{j,1}, x_{j,2})^\top \in \mathbb{R}^2$ the particle coordinates restricted to the two periodic dimensions and set $\tilde{\boldsymbol{L}} := \operatorname{diag}(L_1, L_2)$. A transformation of the long range part into Fourier space with respect to the first two dimensions gives the following result, see [4] and [5].

$$\phi^{\text{long}}(j) = \frac{1}{L_1 L_2} \sum_{\boldsymbol{k}\in\mathbb{Z}^2} \sum_{i=1}^{N} \xi_i \, \mathrm{e}^{2\pi \mathrm{i} \tilde{\boldsymbol{k}}^\top \tilde{\boldsymbol{x}}_{ij}} \Theta^{\text{p2}}\left(\|\tilde{\boldsymbol{k}}\|, x_{ij,3}\right),$$

where we set $\tilde{\boldsymbol{k}} := \tilde{\boldsymbol{L}}^{-1} \boldsymbol{k}$ and the function Θ^{p2} is given by

$$\Theta^{\text{p2}}(k, r) := \begin{cases} \frac{1}{k}\left[\Psi(k, r) + \Psi(k, -r)\right] & : k \neq 0, \\ -\frac{2\sqrt{\pi}}{\alpha} \, \mathrm{e}^{-\alpha^2 r^2} - 2\pi r \operatorname{erf}(\alpha r) & : k = 0, \end{cases}$$

with

$$\Psi(k, r) := \mathrm{e}^{-2\pi k r} \operatorname{erf}\left(\tfrac{\pi k}{\alpha} - \alpha r\right).$$

Note that $\Theta^{\text{p2}}(k, r) = \Theta^{\text{p2}}(k, -r)$, i.e., each function $\Theta^{\text{p2}}(k, \cdot)$ is symmetric. It can be shown easily that for each $r \in \mathbb{R}$ we have $\Theta^{\text{p2}}(k, r) \to 0$ like $\mathcal{O}(k^{-2} \, \mathrm{e}^{-k^2})$ as $k \to \infty$, i.e., the Fourier series converges as fast as in the 3d-periodic case.

C. 1d-periodic boundary conditions

For 1d-periodic boundary conditions regarding the first dimension we have $\mathcal{S} := \mathbb{Z} \times \{0\}^2 \iff p = 1$. In this section we denote by $\tilde{\boldsymbol{x}}_j := (x_{j,2}, x_{j,3})^\top \in \mathbb{R}^2$ the particle coordinates restricted to the two dimensions subject to non periodic boundary conditions. The transformation into Fourier space gives, cf. [6] and [5],

$$\phi^{\text{long}}(j) = \frac{1}{L_1} \sum_{k\in\mathbb{Z}} \sum_{i=1}^{N} \xi_i \, \mathrm{e}^{2\pi \mathrm{i} \tilde{k} x_{ij,1}} \Theta^{\text{p1}}\left(\tilde{k}, \|\tilde{\boldsymbol{x}}_{ij}\|\right),$$

where we set $\tilde{k} := L_1^{-1} k$ and the function Θ^{p1} is given by

$$\Theta^{\text{p1}}(k, r) := \begin{cases} K_0\left(\frac{\pi^2 k^2}{\alpha^2}, \alpha^2 r^2\right) & : k \neq 0, \\ -\left(\gamma + \Gamma(0, \alpha^2 r^2) + \ln(\alpha^2 r^2)\right) & : k = 0. \end{cases}$$

Thereby, we denote by γ the Euler-Mascheroni constant, $\Gamma(s, x) := \int_x^\infty t^{s-1} \, \mathrm{e}^{-t} \mathrm{d}t$ is the upper incomplete Gamma function and $K_0(x, y) := \int_1^\infty t^{-1} \, \mathrm{e}^{-xt - y/t} \mathrm{d}t$ is the incomplete modified Bessel function of the second kind and order zero. The convergence of the Fourier series is as fast as for 3d- and 2d-periodic boundary conditions.

D. 0d-periodic boundary conditions

In the non periodic setting we have

$$\phi^{\text{long}}(j) = \sum_{i=1}^{N} \xi_i \frac{\operatorname{erf}(\alpha\|\boldsymbol{x}_{ij}\|)}{\|\boldsymbol{x}_{ij}\|},$$

i.e., $\mathcal{S} = \{0\}^3 \iff p = 0$. A transformation into Fourier space via the Poisson summation formula is not readily possible.

III. FFT FOR NONEQUISPACED DATA

In the following we give a brief introduction to fast Fourier transforms for nonequispaced data, which are an essential tool for the efficient computation of the introduced interaction quantities between particles, see Section IV.

A. NFFT and adjoint NFFT

The efficient computation of sums of the form

$$f(\boldsymbol{x}_j) = \sum_{\boldsymbol{k}\in\mathcal{I}_{\boldsymbol{M}}} \hat{f}_{\boldsymbol{k}}\, \mathrm{e}^{2\pi \mathrm{i}\boldsymbol{k}^\top \boldsymbol{x}_j}, \quad j = 1,\dots,N,$$

where $\boldsymbol{M} \in 2\mathbb{Z}^d$ and

$$\mathcal{I}_{\boldsymbol{M}} := \big([-\tfrac{M_1}{2}, \tfrac{M_1}{2}) \times \cdots \times [-\tfrac{M_d}{2}, \tfrac{M_d}{2})\big) \cap \mathbb{Z}^d$$

i.e., the evaluation of a trigonometric polynomial f at nonequispaced nodes $\boldsymbol{x}_j \in \mathbb{T}^d \simeq [-1/2, 1/2)^d$, is possible via the so called FFT for nonequispaced data (NFFT), see [7]–[10].

The basic idea behind the approach is to map the unequally spaced nodes $\boldsymbol{x}_j$ onto a regular grid, which is realized via a so called window function. On the equispaced grid we can simply use the well known inverse FFT. Thus, the described approach requires $\mathcal{O}(|\mathcal{I}_{\boldsymbol{M}}| \log |\mathcal{I}_{\boldsymbol{M}}| + N)$ arithmetic operations, which also applies to the different variants, as presented below.

The efficient computation of the sums

$$h(\boldsymbol{k}) = \sum_{j=1}^{N} f_j\, \mathrm{e}^{-2\pi \mathrm{i}\boldsymbol{k}^\top \boldsymbol{x}_j}, \quad \boldsymbol{k} \in \mathcal{I}_{\boldsymbol{M}},$$

follows a similar structure and is based on the well known FFT. The method is widely known as the adjoint NFFT.

B. Further variants in three dimensions

Recently, the NFFT has been generalized in order to evaluate the gradients $\nabla f(\boldsymbol{x}_j) \in \mathbb{C}^3$ (gradient NFFT) as well as the Hessians $\nabla\nabla^\top f(\boldsymbol{x}_j) \in \mathbb{C}^{3\times 3}$ (Hessian NFFT) of a given trivariate trigonometric polynomial f in the unequally spaced nodes $\boldsymbol{x}_j$.

A further variant is called adjoint gradient NFFT, which enables an efficient computation of the sums

$$h(\boldsymbol{k}) := \sum_{j=1}^{N} \boldsymbol{f}_j^\top \nabla_{\boldsymbol{x}}\, \mathrm{e}^{2\pi \mathrm{i}\boldsymbol{k}^\top \boldsymbol{x}}\Big|_{\boldsymbol{x}=\boldsymbol{x}_j} \in \mathbb{C}, \quad \boldsymbol{k} \in \mathcal{I}_{\boldsymbol{M}}.$$

For more details see [3].

C. NFFT based fast summation

In the following we give a short introduction to the NFFT based fast summation approach [11]. We start by considering a one dimensional setting with given nodes $x_j \in [-L/2, L/2]$ and coefficients $\alpha_j \in \mathbb{R}$, $j = 1,\dots,N$. We aim to approximate sums of the form

$$f_j := \sum_{i=1}^{N} \alpha_i K(x_i - x_j), \quad j = 1,\dots,N, \tag{8}$$

where $K : [-L, L] \to \mathbb{R}$ is some continuously differentiable and symmetric function. Note that we have $-L \le x_i - x_j \le L$.

The kernel function K is now embedded into a smooth and periodic function of period $h > 2L$, see Figure 1. The so called regularization is defined via

$$K_{\mathrm{R}}(x) = \begin{cases} K(x) & : x \in [-L, L], \\ K_{\mathrm{B}}(x) & : x \in (L, h-L), \end{cases}$$

where K_{B} is a polynomial, which is constructed such that K_{R} is smooth. This is done by computing the derivatives of K at $x = \pm L$ up to a certain degree of smoothness $p - 1 \in \mathbb{N}$. The polynomial of degree $2p-1$, which fulfills the given interpolation conditions, is found via two point Taylor interpolation, see [12].

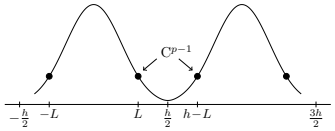

Fig. 1. The regularized kernel function K_{R} is obtained by constructing a smooth transition between L and $h - L$. The obtained periodic function K_{R} is in the space $C^{p-1}(h\mathbb{T})$ for some $p \in \mathbb{N}$.

Since the function K_{R} can be extended to a smooth and h-periodic function, it is well approximated by a trigonometric polynomial. Then, we replace K in (8) by the precomputed approximation to obtain

$$f_j \approx \sum_{l=-M/2}^{M/2-1} \hat{b}_l \left(\sum_{i=1}^{N} \alpha_i \mathrm{e}^{2\pi \mathrm{i} l x_i/h} \right) \mathrm{e}^{-2\pi \mathrm{i} l x_j/h}, \tag{9}$$

where the discrete Fourier coefficients $\hat{b}_l$ are obtained via sampling K_{R} at equispaced nodes in $[-h/2, h/2)$ and applying the FFT. The obtained expressions (9) can be evaluated efficiently as follows. The inner brackets are obtained by applying the adjoint NFFT, followed by a simple multiplication with $\hat{b}_l$. Afterward, the outer sums can be computed by using the NFFT method.

The idea can easily be extended to higher dimensions, where we restrict ourselves to radial kernels, i.e., we replace $K(x_i - x_j)$ by $K(\|\boldsymbol{x}_{ij}\|)$, $\boldsymbol{x}_j \in \mathbb{R}^d$, in (8). The kernel function is regularized based on the one dimensional approach, as presented above, with a slight modification, see Figure 2. Namely, the polynomial K_{B} now lives on the interval $[L, h/2]$ and is claimed to have vanishing derivatives at $x = h/2$.

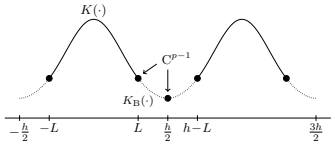

Fig. 2. The function $K_{\mathrm{B}} : [L, h/2] \to \mathbb{R}$ is constructed such that the values of the first $p-1$ derivatives coincide with those of the kernel function K at $x = L$ and that the first $p-1$ derivatives vanish at $x = h/2$.

We obtain a regularization by rotating the resulting one dimensional function, i.e., $K_{\mathrm{R}}(\boldsymbol{x}) := K_{\mathrm{R}}^{1\mathrm{d}}(\|\boldsymbol{x}\|)$ for all $\|\boldsymbol{x}\| \le h/2$. The function is smoothly extended to the cube $[-h/2, h/2]^d$ via $K_{\mathrm{R}}(\boldsymbol{x}) := K_{\mathrm{B}}^{1\mathrm{d}}(h/2)$ for $\boldsymbol{x} \in [-h/2, h/2]^d, \|\boldsymbol{x}\| > h/2$. Since the derivatives are vanishing at the boundaries, the

periodic continuation is smooth, too, and is well approximated by a d-variate trigonometric polynomial with period h in each direction. Thus, we end up with the same structure as in the one dimensional case, see (9).

IV. The P^{2}NFFT method

Based on the Ewald summation formulas, the efficient computation of the electrostatic interactions is more or less straight forward in the 3d-periodic case, cf. [13]. Since the function $r^{-1}\mathrm{erfc}(\alpha r)$ tends to zero exponentially fast for $r \to \infty$, the short range parts (4) can be approximated via direct computation after truncating the infinite sums, i.e., only distances $\|\boldsymbol{x}_{ij} + \boldsymbol{L}\boldsymbol{n}\| \leq r_{\mathrm{cut}}$ for some cutoff radius $r_{\mathrm{cut}} > 0$ are considered. The computation of the self potentials (5) and the $\boldsymbol{k} = \boldsymbol{0}$ parts, see second sum in (6), is possible with only $\mathcal{O}(N)$ arithmetic operations. In order to approximate the Fourier series, see first term in (6), we proceed as follows.

1) Truncate the infinite sum, i.e., replace $\mathbb{Z}^3$ in (6) by a sufficiently large index set $\mathcal{I}_{\boldsymbol{M}}$ with $\boldsymbol{M} \in 2\mathbb{N}^3$.
2) Approximate the structure factors $S(\boldsymbol{k})$, as defined in (7), via the adjoint NFFT and the adjoint gradient NFFT.
3) Multiply with the Fourier coefficients $\hat{\psi}(\boldsymbol{k})$, $\boldsymbol{k} \in \mathcal{I}_{\boldsymbol{M}}$.
4) Compute the outer sums via the NFFT.

In order to compute the forces $\boldsymbol{F}(j)$, see (2), we proceed analogously. Step 4 in the described scheme is replaced by

4c) Compute the outer sums via the gradient NFFT.
5c) Multiply with $-q_j$ for all $j = 1, \ldots, N_{\mathrm{c}}$.

for the charges, cf. [13], [14] for pure charge systems, and by

4d) Compute the outer sums via the Hessian NFFT.
5d) Multiply with $-\boldsymbol{\mu}_j$ from right for all $j = N_{\mathrm{c}}+1, \ldots, N$.

for the dipole particles, cf. [15] for pure dipole systems.

In order to ensure the same accuracy with respect to all three dimensions, the grid size M in step 1 is chosen such that

$$\tfrac{M_1}{L_1} = \tfrac{M_2}{L_2} = \tfrac{M_3}{L_3} \stackrel{!}{=} \beta > 0, \tag{10}$$

i.e., the same resolution is applied in all three dimensions. The described approach requires $\mathcal{O}(N \log N)$ arithmetic operations, provided that the parameters are chosen appropriately.

The computation of the short range as well as the self interactions is done analogously for mixed periodic and open boundary conditions. In order to compute the long range interactions we apply the fast summation approach in the non periodic dimensions, i.e., the 1d fast summation, see Figure 1, is applied for 2d-periodic boundary conditions, and the radial fast summation approach, see Figure 2, is applied in case of 1d-periodicity as well as for open boundary conditions. Thereby, we have to set

$$L := \begin{cases} L_3 & : \text{2d-periodicity}, \\ \sqrt{L_2^2 + L_3^2} & : \text{1d-periodicity}, \\ \sqrt{L_1^2 + L_2^2 + L_3^2} & : \text{0d-periodicity}. \end{cases}$$

The period h is chosen larger than $2L$, i.e., we set

$$h := 2(L + \delta) \quad \text{for some } \delta \geq 0. \tag{11}$$

Based on the fast summation approach for radial kernels in $d = 3$ dimensions, we compute an approximation of the form

$$\frac{\mathrm{erf}(\alpha\|\boldsymbol{x}_{ij}\|)}{\|\boldsymbol{x}_{ij}\|} \approx \sum_{\boldsymbol{l} \in \mathcal{I}_{\boldsymbol{M}}} \hat{b}_{\boldsymbol{l}}\, \mathrm{e}^{2\pi \mathrm{i} \boldsymbol{l}^{\top} \boldsymbol{x}_{ij}/h}$$

for open boundary conditions.

In the mixed periodic settings we have to compute several regularizations. For 2d-periodic boundary conditions we compute the approximations

$$\Theta^{\mathrm{p2}}(\|\tilde{\boldsymbol{k}}\|, x_{ij,3}) \approx \sum_{l=-M/2}^{M/2-1} \hat{b}_{\tilde{\boldsymbol{k}},l}\, \mathrm{e}^{2\pi \mathrm{i} l x_{ij,3}/h}$$

for all $\boldsymbol{k} \in \mathcal{I}_{(M,M)}$ and in case of 1d-periodicity we compute

$$\Theta^{\mathrm{p1}}(\tilde{k}, \|\tilde{\boldsymbol{x}}_{ij}\|) \approx \sum_{\boldsymbol{l} \in \mathcal{I}_{(M,M)}} \hat{b}_{\tilde{k},\boldsymbol{l}}\, \mathrm{e}^{2\pi \mathrm{i} \boldsymbol{l}^{\top} \tilde{\boldsymbol{x}}_{ij}/h}$$

for all $k \in \{-M/2, \ldots, M/2 - 1\}$, cf. [5].

Thereby, the same resolution is used for periodic and non periodic dimensions, see (10). Thus, we choose the cutoff $M \in 2\mathbb{N}$ such that $\frac{M}{h} = \beta$.

Replacing the functions in the presented Fourier space representations by the precomputed trigonometric polynomials, serves the same structure as in the 3d-periodic setting, see fist part in (6). We only have to replace the coefficients $\hat{\psi}(\boldsymbol{k})$ by $\hat{b}_{\boldsymbol{l}}$, $\hat{b}_{\tilde{\boldsymbol{k}},l}$ and $\hat{b}_{\tilde{k},\boldsymbol{l}}$, respectively. We claim that we can obtain approximation errors of a comparable size among all considered types of periodic boundary conditions via the above described parameter choice.

V. Numerical examples

In this section we restrict ourselves to the following setting. We consider small particle systems containing $N_{\mathrm{c}} = 100$ charges $q_j = (-1)^j$ and $N_{\mathrm{d}} = 100$ dipoles with randomly oriented dipole moments $\boldsymbol{\mu}_j \in \mathbb{R}^3$, $\|\boldsymbol{\mu}_j\| = 1$, at random positions $\boldsymbol{x}_j$ in a primary box with edge lengths $L_1 = 8$, $L_2 = 10$ and $L_3 = 12$.

Note that the 3d-periodic case has already been studied in [3]. The presented error estimates enable a tuning of the 3d-periodic Ewald method to a high precision. In order to present a typical error behavior, we consider an above described particle system under 3d-periodic boundary conditions, and compute highly accurate reference data based on the well studied 3d-periodic P^{2}NFFT algorithm. In Figure 3 (top) we plot the measured root mean square (rms) errors in the forces, cf. [3] and references therein, for different parameter combinations. Thereby, we use different near field cutoffs r_{cut} as well as different far field cutoffs β, see (10). Within the NFFT algorithms we use the B-spline of order 8 as window function. Note that the NFFT allows the usage of various other types of window functions. In [16] we achieve even better results with a Bessel function. We further remark that there are basically to approaches in order to compute the partial derivatives within the (adjoint) gradient NFFT and the Hessian NFFT, namely differentiation in Fourier space ($\mathrm{i}\boldsymbol{k}$) and analytic differentiation, see [3] for more details. In the

presented numerical examples we apply the i$\boldsymbol{k}$ differentiation approach.

Now, we consider the same type of particle system subject to open boundary conditions and apply the same parameters. For the fast summation approach we choose the degree of smoothness $p = 10$ and set $\delta := 0.2 \cdot L$ in (11), which results in $h \approx 42.12$. The reference data are simply obtained by evaluating the underlying finite sums directly. The measured rms force errors are plotted in Figure 3 (second row). It can be seen that the errors behave almost the same as in the 3d-periodic example.

We conclude by considering a particle system of the introduced size under 1d-periodic boundary conditions. In order to compute reference data with an rms force accuracy 10^{-10} we evaluate the infinite sums directly, cf. (1). Thereby, we replace the infinite index set $\mathcal{S} = \mathbb{Z} \times \{0\}^2$ by a finite one $\mathcal{S}_C := ([-C, C] \cap \mathbb{Z}) \times \{0\}^2$, where $C \in \mathbb{N}$ is chosen large enough. In order to apply the P^{2}NFFT method for 1d-periodic boundary conditions, we choose the degree of smoothness $p = 10$ and set $\delta := 0.3 \cdot L$ in (11), i.e., $h \approx 40.61$. The measured rms force errors are plotted in Figure 3, too. We obtain errors, which are of a comparable size, compared with those of the 3d-periodic example.

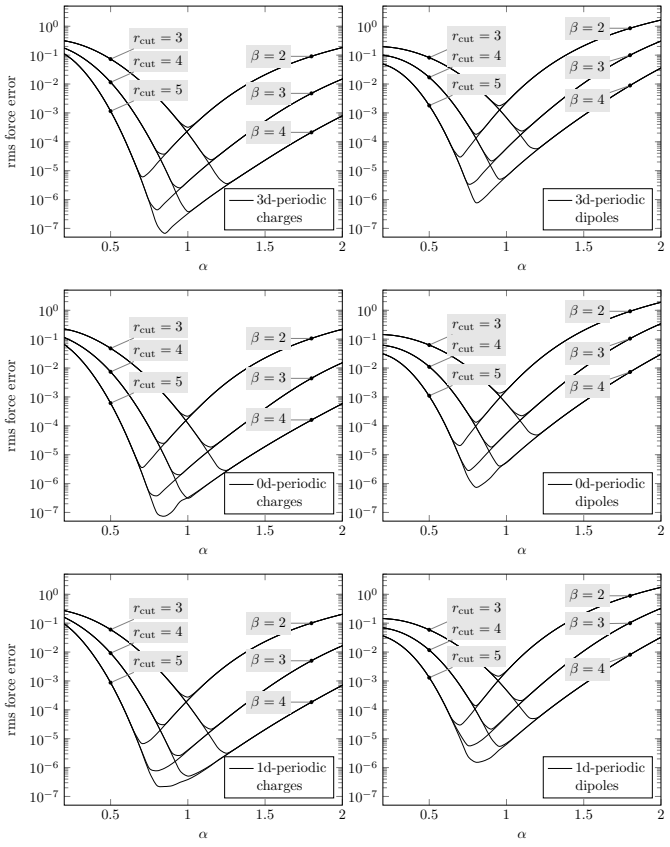

Fig. 3. Rms force errors for the charges (left) and for the dipoles (right) with respect to the splitting parameter α for different combinations of the near field cutoff r_{cut} and the far field cutoff β (see labels), 3d-periodic (top) 0d-periodic (middle) and 1d-periodic (bottom).

VI. Conclusion

In this paper we gave a short introduction to the P^{2}NFFT method, which is publicly available as a part of the ScFaCoS library [17] and has recently been generalized for the treatment of particle systems containing both point charges as well as point dipoles. The combination of the Ewald summation formulas and the NFFT based fast summation enables a unified treatment of fully periodic, partially periodic as well as open boundary conditions. We presented for the first time numerical examples for open as well as mixed periodic boundary conditions, showing that the method can be tuned to a high precision.

Acknowledgment

The author gratefully acknowledges support by the German Research Foundation (DFG), project PO 711/12-1. Furthermore, the author would like to thank M. Pippig and M. Hofmann for their support regarding the implementation and C. Holm as well as the members of his working group for fruitful discussions.

References

[1] S. W. de Leeuw, J. W. Perram, and E. R. Smith, "Simulation of electrostatic systems in periodic boundary conditions. I. Lattice sums and dielectric constants," *Proc. R. Soc. Lond. Ser. A Math. Phys. Eng. Sci.*, vol. 373, pp. 27–56, 1980.

[2] P. P. Ewald, "Die Berechnung optischer und elektrostatischer Gitterpotentiale," *Ann. Phys.*, vol. 369, pp. 253–287, 1921.

[3] M. Hofmann, F. Nestler, and M. Pippig, "NFFT based Ewald summation for electrostatic systems with charges and dipoles," *Preprint 2016-07, Faculty of Mathematics, Technische Universität Chemnitz*, 2016.

[4] A. Grzybowski, E. Gwóźdź, and A. Bródka, "Ewald summation of electrostatic interactions in molecular dynamics of a three-dimensional system with periodicity in two directions," *Phys. Rev. B*, vol. 61, pp. 6706–6712, 2000.

[5] F. Nestler, M. Pippig, and D. Potts, "Fast Ewald summation based on NFFT with mixed periodicity," *J. Comput. Phys.*, vol. 285, pp. 280–315, 2015.

[6] M. Porto, "Ewald summation of electrostatic interactions of systems with finite extent in two of three dimensions," *J. Phys. A*, vol. 33, pp. 6211–6218, 2000.

[7] A. Dutt and V. Rokhlin, "Fast Fourier transforms for nonequispaced data," *SIAM J. Sci. Stat. Comput.*, vol. 14, pp. 1368–1393, 1993.

[8] G. Beylkin, "On the fast Fourier transform of functions with singularities," *Appl. Comput. Harmon. Anal.*, vol. 2, pp. 363–381, 1995.

[9] G. Steidl, "A note on fast Fourier transforms for nonequispaced grids," *Adv. Comput. Math.*, vol. 9, pp. 337–353, 1998.

[10] A. J. W. Duijndam and M. A. Schonewille, "Nonuniform fast Fourier transform," *Geophysics*, vol. 64, pp. 539–551, 1999.

[11] D. Potts and G. Steidl, "Fast summation at nonequispaced knots by NFFTs," *SIAM J. Sci. Comput.*, vol. 24, pp. 2013–2037, 2003.

[12] M. Fenn and G. Steidl, "Fast NFFT based summation of radial functions," *Sampl. Theory Signal Image Process.*, vol. 3, pp. 1–28, 2004.

[13] M. Pippig and D. Potts, "Parallel three-dimensional nonequispaced fast Fourier transforms and their application to particle simulation," *SIAM J. Sci. Comput.*, vol. 35, pp. C411–C437, 2013.

[14] J. Eastwood, R. Hockney, and D. Lawrence, "P3M3DPThe three-dimensional periodic particle-particle/ particle-mesh program," *Computer Physics Communications*, vol. 19, no. 2, pp. 215 – 261, 1980.

[15] J. J. Cerdà, V. Ballenegger, O. Lenz, and C. Holm, "P3M algorithm for dipolar interactions," *J. Chem. Phys.*, vol. 129, p. 234104, 2008.

[16] F. Nestler, "Parameter tuning for the NFFT based fast Ewald summation," *Front. Phys.*, vol. 4, no. 28, 2016.

[17] A. Arnold, M. Bolten, H. Dachsel, F. Fahrenberger, F. Gähler, R. Halver, F. Heber, M. Hofmann, J. Iseringhausen, I. Kabadshow, O. Lenz, and M. Pippig, "ScaFaCoS - Scalable Fast Coloumb Solvers," http://www.scafacos.de.